



UNIVERSITY OF LEEDS

This is a repository copy of *Amphiphilic Block Copolymers for Flocculation and Hydrophobization of Legacy Waste Suspensions in Flotation Driven Dewatering Operations*.

White Rose Research Online URL for this paper:
<http://eprints.whiterose.ac.uk/160860/>

Version: Accepted Version

Proceedings Paper:

Lockwood, A, Wadsley, G, Warren, N et al. (5 more authors) (2020) Amphiphilic Block Copolymers for Flocculation and Hydrophobization of Legacy Waste Suspensions in Flotation Driven Dewatering Operations. In: WM Symposia 2020. Waste Management Symposium 2020, 08-12 Mar 2020, Phoenix, Arizona. .

Copyright © by WM Symposia. All Rights Reserved. Reprinted with permission. This is an author produced version of a conference paper published in WM Symposia 2020. Uploaded in accordance with the publisher's self-archiving policy.

Reuse

Items deposited in White Rose Research Online are protected by copyright, with all rights reserved unless indicated otherwise. They may be downloaded and/or printed for private study, or other acts as permitted by national copyright laws. The publisher or other rights holders may allow further reproduction and re-use of the full text version. This is indicated by the licence information on the White Rose Research Online record for the item.

Takedown

If you consider content in White Rose Research Online to be in breach of UK law, please notify us by emailing eprints@whiterose.ac.uk including the URL of the record and the reason for the withdrawal request.



eprints@whiterose.ac.uk
<https://eprints.whiterose.ac.uk/>

Amphiphilic Block Copolymers for Flocculation and Hydrophobization of Legacy Waste Suspensions in Flotation Driven Dewatering Operations - 20162

Alexander P. G. Lockwood*, Georgina Wadsley*, Nicholas J. Warren*, David Harbottle*, Timothy N. Hunter*, Jeffrey Peakall**, Geoff Randall***, Martyn G. Barnes***

* School of Chemical and Process Engineering, University of Leeds, LS2 9JT, United Kingdom

** School of Earth and Environment, University of Leeds, LS2 9JT, United Kingdom

*** Centre of Sludge Expertise, Sellafield Ltd, Birchwood, WA3 6GR

ABSTRACT

Flotation has been effectively demonstrated as a low footprint, high efficiency separation process when utilising simple anionic surface modifying agents such as sodium dodecyl sulphate (SDS). These agents increase hydrophobicity to remove suspended cationic surface charged particulates such as $Mg(OH)_2$ from waste suspensions similar to those at British nuclear fuel management sites- where corrosion processes have degraded fuel cladding. The technology is advantageous as it could effectively be retrofitted into existing waste management facilities at nuclear waste management sites such Sellafield and Hanford as the simplicity (no moving parts) and size of this technology coupled with low cost of construction could be rapidly deployed to aid in risk and hazard reduction decommissioning operations with minimum impact to secondary waste generation. Previously, sodium dodecyl sulphate has been deployed as a collector agent to increase the hydrophobicity of $Mg(OH)_2$ suspended particles, achieving a maximum particulate extraction percentage of 93%. To achieve further particulate extraction, flotation performance has been determined to be a function of the hydrodynamic limitations extracting fine material ($>20 \mu m$). Fine particulates have been shown in the minerals industry to have an inability to overcome slipstreams created from rising bubbles in flotation cells, likely due to the low mass and thus momentum of the colloidal material, preventing interaction between the hydrophobized particles and air-water interfaces (bubbles). To combat this mass transfer resistance poly(acrylic acid)-block-poly(n-butyl acrylate) amphiphilic diblock copolymers were synthesised via reversible addition-fragmentation chain-transfer (RAFT) polymerisation. The anticipated mode of action of these polymers involves the hydrophilic poly(acrylic acid) block polymer acting as a flocculation agent to increase the mass of the aggregates, and the hydrophobic poly(n-butyl acrylate) modifies the hydrophobicity of the resulting flocs. The concentration of this polymer (termed a macro-collector) was varied and the change in particle size distribution of the particulate suspension was analysed using static light scattering. The flotation performance was then characterised by several methods including percentage particulate recovery, volume reduction factor and residual bulk particulate concentration. This was then benchmarked against the traditional surfactant collector agent SDS.

INTRODUCTION

The UK's incipient civil nuclear campaign saw the commission of the first-generation Magnox storage pond (FGMSP), a large outdoor fuel storage facility for Magnox reactor fleet fuel. Intended to be temporary storage for the bespoke Magnox clad fuel (an alloy of primarily magnesium, 0.7% aluminium and 5ppm beryllium)[1], the open-air nature of the facility has been subject to external contaminants resulting in a restricted ability to control pond water chemistry[2]. This combined with the extended storage period has resulted in the extensive corrosion of the Magnox cladding as illustrated in figure 1. FGMSP is understood to be contaminated with approximately 1400m³ of Mg(OH)₂ based sludge material[3], [4], with the presence of fuel rod fragments, metal fragments (from fuel skips), concrete degradation products (from the pond infrastructure), wind-blown sand, and other materials such as bird guano and animal remains as illustrated in Figure 1[1]. This has resulted in the release of radionuclides raising activity levels in pond water to ~1000 TBq.m⁻³ [5]. The corrosion process has additionally led to the production of Mg(OH)₂ colloidal material. Maher et al.[6] found that due to the colloidal material's small size and high surface area to mass ratio- Mg(OH)₂ brucite is a potential controller of radionuclide speciation, capable of incorporating radionuclides (particularly the actinides) into their structure such as Pu⁵⁺ and Am³⁺. These colloids produce a vector for the incorporated radionuclides to proceed through downstream ion exchange processes unabated. Mg(OH)₂ also dissolves at pH ~7 in the carbonation stage of the ion exchange process producing competing ions which reduce the effectiveness of the clinoptilolite ion exchange media in reducing the ¹³⁷Cs and ⁹⁰Sr discharge concentrations[7].

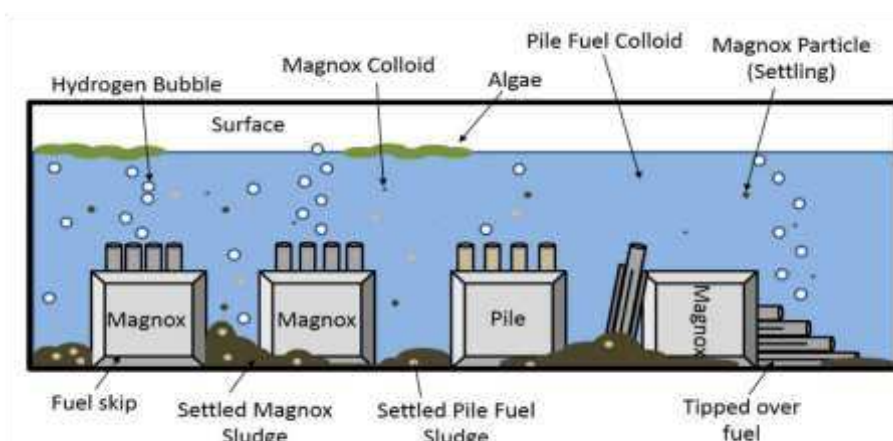


Fig. 1. Illustration of the First-Generation Magnox Storage Pond with associated decommissioning challenges including the presence of corroded Magnox sludge, suspended colloidal material, corrosion driven hydrogen production, tipped fuel skips and algal contamination.

Due to FGMSPs complex contamination, Sellafield Ltd. has placed this facility under an extensive risk and hazard reduction programme named additional sludge retrieval (ASR)[8]. To remove the corroded Mg(OH)₂ sludge material, the FGMSP dedicated sludge packaging plant 1 (SPP1) has been deployed. The dewatering mechanism of SPP1, a gravitational thickener such as those used in the minerals and water treatment industries[9]–[12], relies on gravity driven sedimentation for separation of solid Mg(OH)₂ material and returning the resultant cleared supernatant liquor back to FGMSP. However, gravity sedimentation of colloidal particulates has been shown to be ineffective, especially when the low surface potential of Mg(OH)₂ (~+12 mV[13]) results in naturally aggregating material. Johnson et al.[14] found in an investigation into the hindered sedimentation of Mg(OH)₂ that this aggregation results in open structures which display lower aggregate densities (1059-1081 kg.m⁻³). The lower effective densities coupled with low mass of the colloidal material in a hindered settling regime requires

extensive sedimentation residence times for adequate removal of suspended material from the supernatant.

A typical solution for improving the dewatering performance of hindered settling systems in thickeners is to deploy polymeric flocculants[9], [15]–[19]. These flocculation agents are often large molecular weight (MW) statistical or random copolymers (MW~ 10^6 g/mol), comprising of a charged monomer (opposite charge to the particle surface), and a non-ionic monomer, where the concentration ratio of each determines the overall polymer charge density[9]. These larger, lower charge density (10-40% ionic monomer) polymers have slower surface conformation rates when adsorbing to a particulate surface. This slower conformation allows the polymer chains to extend beyond the Debye layer of the particulate[15], [16]. This non-adsorbed polymer adsorbs onto adjacent particles forming a low density floc with a much larger hydrodynamic radii ($d_{50} > 100 \mu\text{m}$)[18] than naturally aggregated $\text{Mg}(\text{OH})_2$, thus increasing the zonal sedimentation rate of the suspension[18]–[20]. An alternative flocculation mechanism is to deploy lower molecular weight homopolymers comprising one charged monomer which are highly mobile and form a tight polymer conformation and localised charge reversal resulting in charge patch neutralisation flocculation[21]. An investigation by Zhou and Franks[21] found that increasing the charge density of polymers resulted in denser flocs with smaller hydrodynamic radii than the lower charge density polymer systems, which produced larger more porous flocs containing more embodied water due to their open structure[22] as depicted in Figure 2. However, polymeric flocs are prone to breakdown in shear conditions[21], [23]–[27]. SPP1 has been constructed with a pipe bridge linking the facility to FGMSP. Slurry is sent to SPP1 in batches of 80 m^3 (including flushing of the slurry lined with pond water)[8] and a consequence of transporting these suspensions effectively requires that pumping velocities be above the suspension's critical deposition velocity. Axiomatically, these suspensions are subject to high shear conditions reducing floc hydrodynamic radii and dewatering performance as previously investigated[21], [23]–[27].

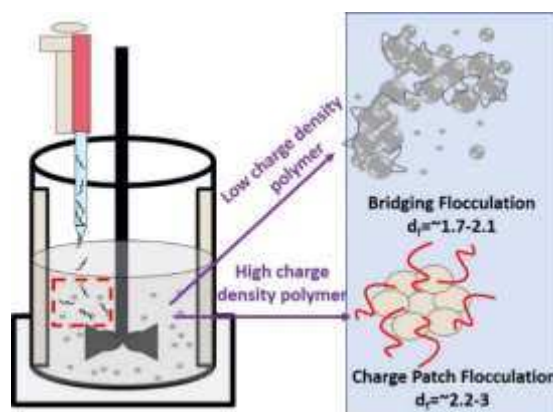


Fig. 2. Illustration of bridging and charge patch neutralisation flocculation mechanisms.

Flotation was selected as an alternative dewatering technology as it is recognised as a low footprint, high efficiency cationic particulate separation process when utilising simple anionic surface modifying agents. Additionally the rapid nature of the process has lower process residence times than those observed in gravity driven sedimentation particularly in algal rich waters[28]. Surface modifier agents known as collectors, are often surfactants- molecules which have a charged head group and hydrophobic alkyl chain tails. The amphiphilic properties of surfactants allow adsorption to air-water interfaces and reduction of interfacial surface tension increasing foaming.

The surfactant head groups adsorb to the oppositely charged particle surface forming a monolayer where the outward facing hydrophobic tails increase particulate wettability and particle hydrophobicity (see

Figure 3). These modified particles actively adsorb to air-water interfaces, which in flotation manifests as rising bubbles. Post bubble attachment, the modified particles are transported to the foam phase via buoyancy, where the particulate loaded foam phase can be separated from the bulk suspension via a foam skim as illustrated in figure 3.

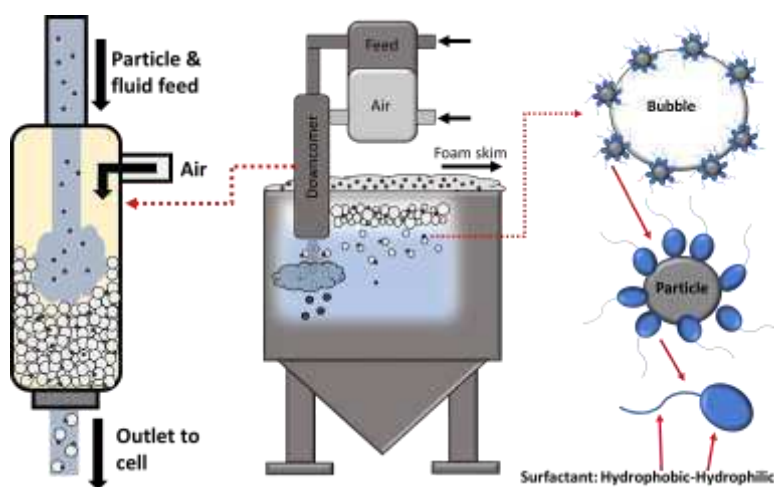


Fig. 3. Illustration of a flotation cell such as the Jameson Cell.

Lockwood et al.[13] previously investigated flotation of $Mg(OH)_2$ suspensions using a sodium dodecyl sulphate (SDS) collector agent with a methyl isobutyl carbinol (MIBC) frothing agent. Particulate recovery percentages as high as 93% were achieved but large amounts of water carryover were also observed. Flotation performance data combined with adsorption isotherm analysis indicated it was likely only a proportion of particulates were recovered via hydrophobization mechanisms (adsorbing to the air-water interface). Excess surfactant concentrations resulted in increased foaming and fluid entrainment, where the homogeneously mixed suspension axiomatically contains additional particulates[13]. Smaller particulates have been found in literature to have the inability to interact with the air-water interfaces in flotation due to the slip stream created by rising bubbles[29]. The lack of mass and thus inertia to overcome this hydrodynamic barrier prevents hydrophobically driven separation. Particle size flotation performance envelopes vary in flotation literature but are often approximated as being between ~ 20 - $150 \mu m$ [30]–[32], where smaller particulates lack inertia and larger particulates gravitationally overcome air bubble buoyancy. Additional investigations in fine and coarse particle flotation by Gontijo et al.[33] found that the stability of the bubble-particle aggregate controls the maximum floatable particle size of coarse particles, and for fine particles the flotation limit is dictated by the energy required to rupture the intervening liquid film between the particle and bubble. As it has been identified that the smaller particulates are primarily responsible for not only incorporating radionuclides but also being the likely vectors for abatement avoidance[6], additional dewatering stages must be incorporated for this process to be effective in reducing radionuclide discharge to the Irish sea.

For increased extraction of fine particulates, a combination of flocculation and increasing the hydrophobic surface modification functionality is required. Temperature responsive polymers have been investigated in depth as summarised in a review by Ng et al.[29], which compared the performance of a range of different types of polymers-primarily poly(*n*-isopropyl acrylamide), a temperature responsive polymer that becomes hydrophobic above its lower critical solution temperature (LCST)[29]. This polymer was used as both a mono-polymer collector and was copolymerized in various research to make copolymers incorporating the monomers: acrylic acid (anionic) and ethyl xanthate methacrylate (cationic)[34], [35]. These temperature responsive polymers were used to separate a range of minerals however, due to the cationic nature of $Mg(OH)_2$ as quantified by Lockwood

et al.[13] and Johnson et al.[14] analogous minerals, such as alumina, hematite and vale iron ore, as well as anionic copolymers are of particular interest. Generally, these dual flocculation-collector reagents have been shown to be effective, particularly in the extraction of hematite using poly(acrylic acid)-co-poly(n-isopropyl acrylate) where a significant enhancement in the recovery of fine hematite particles below 20 μm was observed for both hematite/quartz mixtures and vale iron ore[29], [36]. This recovery ceases to be selective for particles sized at 1 μm and below for both systems. This sub-micron lower selectivity phenomenon was attributed to gangue entrapment inside the hydrophobic flocs resulting in concentrate dilution. The presence of these anionic copolymers on the surfaces of cationic mineral particles significantly increases the probability of attachment to air-water interfaces leading to an overall selective increase in particle floatability[35]. However, heating large volumes of suspensions above their LCST is economically inefficient and temperature variations in systems may cause issues with the British nuclear regulatory body as the corrosion process not only produces hydrogen but in the case of extensive evaporation, risks igniting pyrophoric fuel[37].

While previous investigations of large statistical copolymers have been found to be effective utilising bridging flocculation, the incorporated gangue material in their open structures have proven problematic. As only solid-liquid separation is required for this decommissioning campaign with no criteria for selectivity unlike the minerals industry, the use of non-responsive block copolymers can be considered as an alternative flocculation-collector agent. In contrast to statistical polymers - which have a random probabilistic arrangement of adjacent monomer units (e.g. ABABAABA)- block copolymers have a sectional block arrangement of adjacent monomers (e.g. AAAABBBB). The segregation of monomers in these amphiphilic polymers gives these molecules surface active properties, essentially acting as macromolecular-surfactants (or macro-surfactants). These polymers also display self-assembly characteristics forming micelles to reduce free energy of the system as observed by Colombani et al.[38] who investigated the critical micelle concentration (CMC) of poly(acrylic acid)-block-poly(n-butyl acrylate) [PAA-b-Pn-BA].

A function of a segregated hydrophilic charged group with 100% anionic charge density is that due to the rapid and dense conformation of the charge groups to a particle surface, the polymer would likely promote areas of localised charge neutralisation and reversal inducing charge patch flocculation in cationic suspension[15], [21]. This mechanism, depicted in Figure 4, would likely form smaller and denser flocs as indicated in the work by Zhou and Franks[21], which may minimize the gangue entrapment reported when utilising the larger temperature responsive PNIPAM-PAA copolymers in the work of Ng et al.[36] and Forbes et al.[35] thus improving the dewatering capability of these systems by reducing concentrate dilution[29]. The relative molecular lengths of hydrophobic and hydrophilic chain groups have been found to affect surface activity and particle self-assembly, whereas the hydrophilic group molecular weight will affect adsorption density and flocculated particle size distribution. The density of polymer adsorption will axiomatically control the density of hydrophobic chains present on the floc surface which will dictate the floc contact angle. The investigation into the limits of fine and coarse particle flotation by Gontijo et al.[33] recommends that for optimum flotation the contact angle of a particle should be maximised. Building on this logic, it is known from the work of Evans et al.[39] that for carboxylate surfactant flotation, the chain length of the hydrophobic blocks directly increases hydrophobicity with increasing length, the caveat of increasing the chain lengths for these surfactants and block copolymers is that it will lower the CMC[38].

Whilst micellar adsorption is possible and will likely still promote flocculation, it will act as a poor surface modifier due to the protected hydrophobic chains.

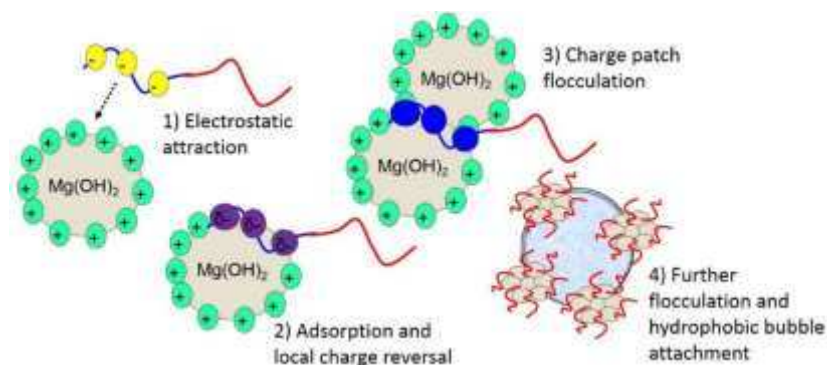


Fig. 4. Diagram of alternative collector mechanism to traditional surfactant flotation- diblock amphiphilic polymer utilising a dual charge patch neutralisation flocculation-surface modification functionality mechanism to increase particle size and hydrophobicity for enhanced extraction in flotation operations.

This research aims to investigate the effectiveness of the amphiphilic block copolymer PAA-b-PnBA use in the flocculation and hydrophobization of $\text{Mg}(\text{OH})_2$ 2.5 vol% suspensions in batch flotation operations. The relative chain length of the hydrophilic anionic PAA block was selected to have a constant degree of polymerization (D_p) ~ 160 ($\text{MW} \sim 10^4 \text{g/mol}$) with two different hydrophobic chain lengths for the hydrophobic PnBA blocks of $D_p=25$ and $D_p=200$. The solution properties of these block copolymers were compared by investigating the change in surface tension with varying concentration polymer solutions using tensiometry. Their flocculation performance was then characterised by analysis of the fractal structure of the resultant flocs using static light scattering (SLS) and finally a direct comparison of flotation performance regarding the mass percentage recovery, volume reduction factor and residual cell particulate concentrations. The polymer performances were then benchmarked against the performance of SDS in flotation of 2.5 vol% $\text{Mg}(\text{OH})_2$ previously investigated in the work of Lockwood et al.[13] to compare the effectiveness of different collector mechanisms.

MATERIALS & METHODOLOGY

Raw Materials

$\text{Mg}(\text{OH})_2$ (Versamag, Martin Marietta, US) was used for flocculation and flotation experiments and was analysed using a Malvern Mastersizer 2000E to have a particle d_{50} of 2.44 μm . Versamag is a fine white precipitated powder with a solubility of 6.9 mg.l^{-1} in water[40]. Researching the same material as previous work, Lockwood et al.[13] summarised the material properties in Table I. $\text{Mg}(\text{OH})_2$ is made up of aggregates of pseudo-hexagonal platelets similar to those reported by Johnson et al. [14] and Maher et al.[6]. Surface charge analysis found the ζ -Potential (mV) to be ~ 12 mV indicating cationic surface charge with a specific surface area of $\sim 7.6 \text{m}^2\text{g}^{-1}$ analysed using a BET isotherm with specific nitrogen adsorption. The material also self-buffered due to its semi soluble nature maintaining a suspension pH of 10.10 for a solids concentration of 2.5 vol%.

Table I. Physical characteristics of $\text{Mg}(\text{OH})_2$ suspended in Milli-Q water at 2.5% v/v, as summarised by Lockwood et al.[13].

Species	D[0.5](μm)	ζ -Potential (mV)	BET S.A. (m^2g^{-1})	pH
$\text{Mg}(\text{OH})_2$	2.45 ± 0.31	12.03 ± 0.03	7.56 ± 0.17	10.10 ± 0.26

Sodium Dodecyl Sulphate (SDS) pellets (TOKU_E $\geq 99\%$) were dissolved in 0.5 l of milli-Q water to make up a collector agent bulk solution of 16.4 mM which was stored in a polypropylene container previously washed with Decon-90, then rinsed with ethanol to disperse any remaining surfactants, rinsed with milli-Q water and dried in an oven to remove any moisture. This bulk solution was diluted with milli-Q water accordingly for experiments[13]. A frother stock solution of 100 ppm concentration was made using 4-methyl-2-pentanol (MIBC) (Sigma-Aldrich, 98%) and milliQ water. MIBC was used as a frothing agent for floatation experiments to produce the foam phase[13], [41].

Diblock Copolymer Synthesis

Colombani et al.[38] previously synthesised PAA-b-PnBA diblock copolymers using Atom transfer radical polymerization (ATRP). Here, we elected to use Reversible addition–fragmentation chain-transfer (RAFT) polymerization which has been proven as an effective controlled radical polymerization process that features aspects of living polymerization whilst also gaining from the versatility of a radical polymerisation process. The RAFT process enables the synthesis of diblock copolymers exhibiting predictable molecular weight, low molar mass dispersity (\mathcal{D}), high end-group fidelity, and capacity for continued chain growth[42], [43]. The overall process in this work involved first synthesising a PAA macromolecular chain transfer (macro-CTA) by solution RAFT of acrylic acid (AA) in water (see Figure 5a), then subsequently chain extended with n-butyl acrylate (nBA) via RAFT emulsion polymerisation in water (see Figure 5b). The latter process has been well reported recently and is beneficial in that it enables aqueous polymerisation of insoluble monomers.

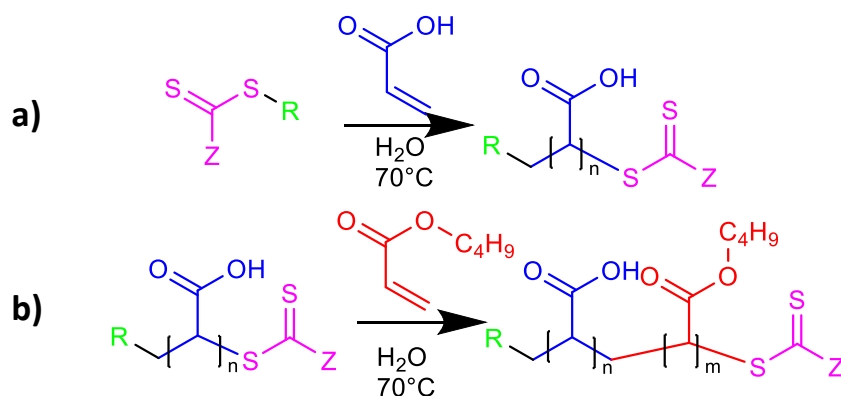


Fig. 5. Diblock polymer RAFT reaction scheme where the top reaction (a) is the synthesis of the poly(acrylic acid) macro chain transfer agent and the bottom reaction (b) is the poly(n-butyl acrylate) diblock attachment reaction carried out in an inert N_2 atmosphere at 70°C . The reaction was carried out in a H_2O solvent media with ACVA initiator and CCTP chain transfer agent.

Acrylic acid (AA; Acros Organics 99.5% extra pure stabilised) was polymerised to form a macro-CTA, which as shown in Figure 5a, is required for synthesis of the diblock copolymers.

A degree of polymerisation of 160 ($\text{Dp}=160$) and solids concentration of 30 weight% were the targeted product of polymerisation. The polymerisation initiator 4,4'-Azobis(4-cyanovalric acid) [ACVA] (Merck $\geq 75\%$) and chain transfer agent 3-(((1-carboxylethyl)thio)carbonothioyl)thio)propanoic acid (CCTP; Boron Molecular) were used in a molecular ratio of initiator: CTA: monomer of 0.4:1:160 respectively, diluted in the required volume of milli-Q water to achieve 30 weight% solids concentration. The polymer reagents were formulated and gently agitated with a magnetic stirrer for 2 hours to ensure full reagent dissolution. The resultant aqueous polymer mixture was then transferred to a 250 ml round bottom flask containing a magnetic stirrer bar and sealed with a rubber septum with a needle exhaust as

an outlet for excess nitrogen during purging. A second needle connected to a nitrogen supply was inserted into the septum and the tip submerged in the aqueous polymer mixture reaction solution. The reaction solution was then placed on a magnetic stirrer operating at 500 rpm. Nitrogen was then sparged into the vessel directly into the liquid phase for 1 hour. Once sufficiently purged, the reaction was initiated by placing the round bottom flask polymer mixture into a paraffin oil bath heated at 70°C and stirred at 500 rpm under a nitrogen atmosphere with the nitrogen inlet raised above that of the liquid into the headroom of the flask. To monitor the polymerisation, 0.4 ml aliquots were extracted from the reaction vessel using a degassed syringe fitted with a needle and placed into NMR tubes at 2-minute intervals for the first 10 minutes, then at increasingly sparse intervals up to 60 minutes. The aliquots were analysed using a Magritek® ¹H Spinsolve 60 MHz Carbon benchtop NMR spectrometer. The series of NMR spectra in Figure 6A show the appearance of broad peaks due to the polymer formation. By integrating the peaks due to formation of PAA ($\delta=0.1$ ppm to 2.9 ppm) and the vinyl proton peaks ($\delta=6.5$ ppm to 5.1 ppm) from each spectrum, the monomer conversion was calculated as a function of reaction time, where the conversion of monomer at time t is $X_{AA}=1 - A_t/A_0$, where A_t and A_0 are the ratios of the monomer to PAA in the NMR spectra at t_t and t_0 respectively[38]. Figure 6B shows a final monomer conversion $X_{AA}= 95\%$ was attained. From the conversion data, a semi-logarithmic plot ($\ln[A_0]/[A]$ vs time) was constructed (Figure 6B) which indicated a deviation from the expected pseudo-first order kinetics beyond ~ 90% conversion. The reaction was stopped by removing the round bottom flask from the paraffin oil bath and exposing the aqueous polymer mixture to the atmosphere.

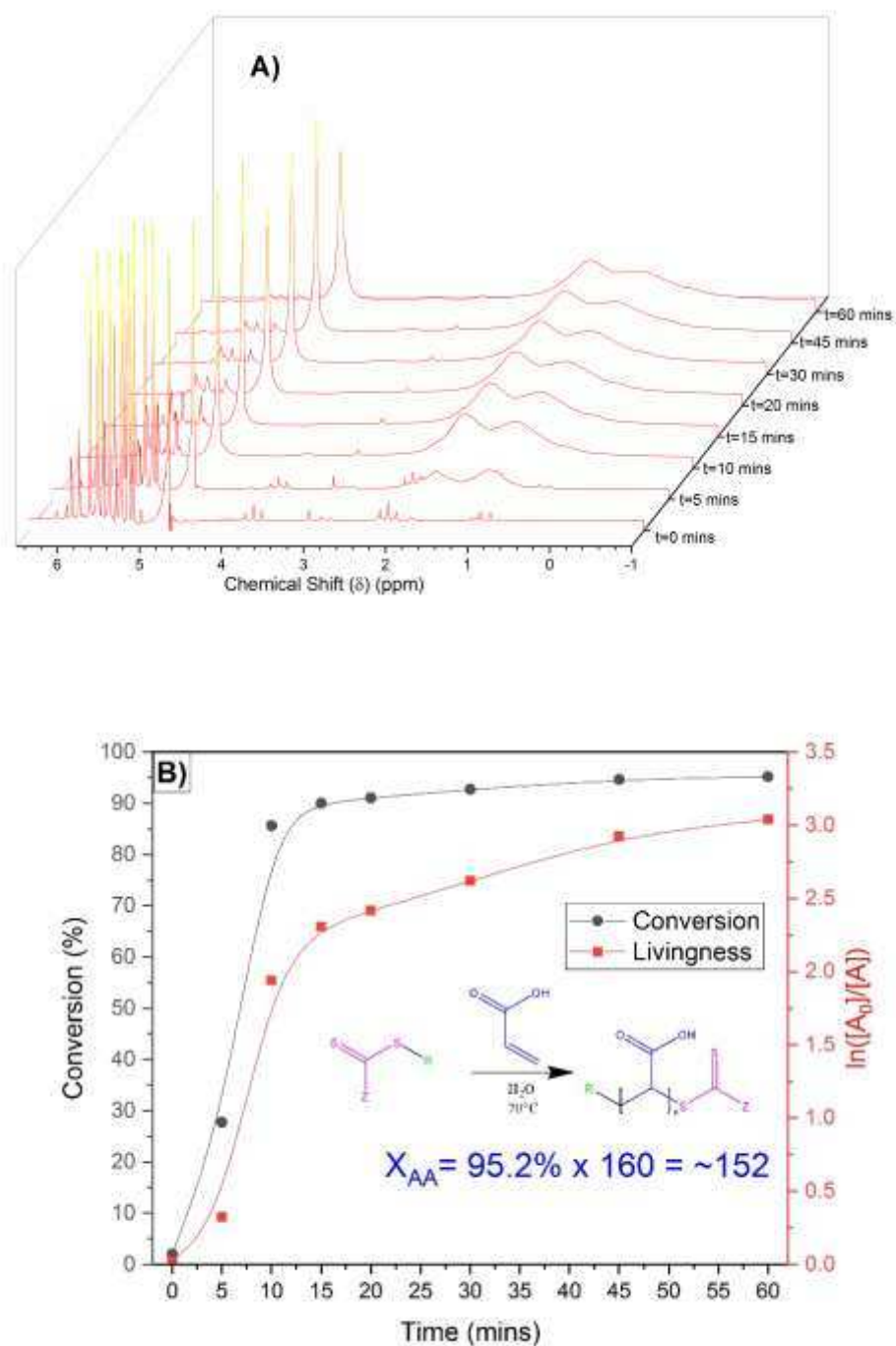


Fig. 6. A) NMR waterfall spectra plot evolution with time for the synthesis of poly(acrylic acid) macro-CTA B) Conversion of acrylic acid to poly(acrylic acid) as a function of time and polymer livingness.

The macro-CTA PAA₁₅₂ was then directly used in the synthesis of the diblock without further purification (as a 30% w/w solution). The diblock copolymer was synthesised by polymerizing nBA (VWR >98%, stab. with up to 50ppm 4-methoxyphenol ml) using ACVA as the initiator and the previously synthesised PAA₁₅₂ as a macro-CTA. The molecular ratio for the two target polymers for initiator: macro-CTA: monomer was 0.4:1:25 for the first diblock copolymer PAA₁₅₂-b-PnBA₂₅

($D_p=25$) and 0.4:1:200 for the second diblock copolymer PAA₁₅₂-b-PnBuA₂₀₀ ($D_p=200$). The reaction procedure was the same as for the PAA₁₅₂ synthesis, but differed regarding sampling, characterisation and reaction time. Unlike the synthesis of the macro-CTA, maximum conversion was preferably required. To achieve this high conversion, the reaction residence time was extended to 3 hours to ensure completion. During this reaction, there was an increase in viscosity due to interactions between the amphiphilic chains. This resulted in difficulty extracting aliquots from the reaction vessel without using a needle gauge that compromised the integrity of the suba-seal. Therefore, the polymer was characterised ex situ. Due to the immiscibility of nBA and water, the mixture was dissolved in 90% methanol. Integration of the relevant peaks in the spectrum was difficult in this case due to overlap between polymer and methanol ($\delta=0.1$ ppm to 2.9 ppm). Therefore, an NMR standard, 3-(trimethylsilyl)-1-propanesulfonic acid sodium salt (TMS salt; Sigma Aldrich; 99%) with peaks around $\delta = 0$ ppm, was added into the reaction (0.4 g/g solid polymer). The peaks from the TMS salt could then be compared with the depletion of those from the vinyl protons in the monomer. A presaturation solvent suppression technique was also used to reduce the magnitude of methanol peaks in the spectra for ease of analysis. The conversion was calculated to be >99% as final vinyl peak integrals were within the noise of the bench top NMR instrument as shown in figure 7. The targeted and achieved block lengths for the two synthesised polymers are summarised below in table 2.

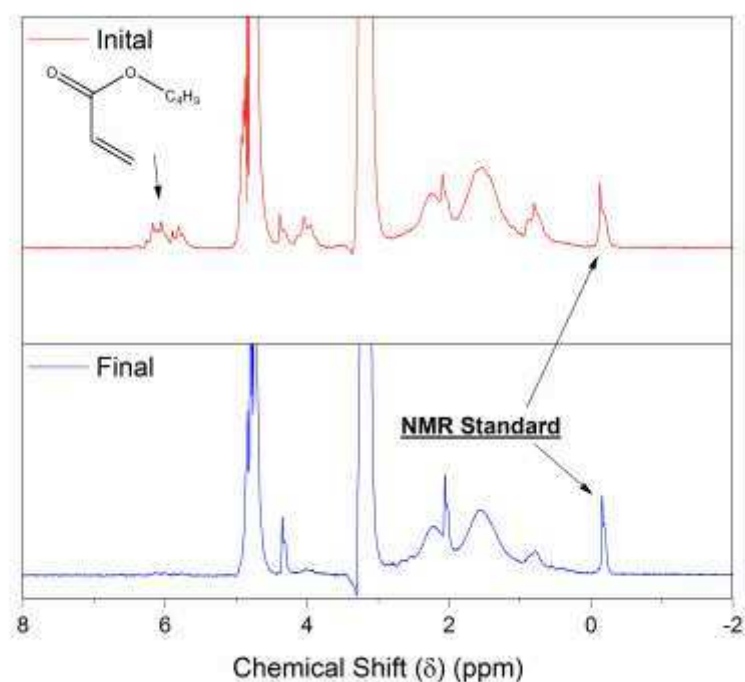


Fig. 7. NMR spectra of PAA-b-PnBA diblock copolymer at the beginning and end of reaction with highlighted TMS salt and vinyl proton environments peaks.

Table II. Summary of target diblock copolymers and achieved degrees of polymerisation and resultant block lengths.

Target Polymer	PAA Actual Dp	PnBA Actual Dp	X _{nBA}
PAA ₁₆₀ -b-PnBA ₂₅	152	25	>99%
PAA ₁₆₀ -b-PnBA ₂₀₀	152	200	>99%

Experimental Methodology

Surface tension analysis

The surface tension of various concentrations (25 ppm-3000 ppm) of the two synthesised diblock copolymers were investigated using pendant drop surface tension analysis performed by using the industry standard image analysis tensiometry instrument Attension Theta (Biolin Scientific, Sweden). The instrument camera takes photos of the water drop (at air-water equilibrium surface tension of the diblock copolymers using an automated syringe) and transmits the images to the tensiometer's bespoke computer-software for analysis. The software then determines a numerical solution for the surface tension using the Young-Laplace equation (equation 1), where γ is the liquid surface tension (for liquid-air surface), ΔP is the pressure difference across the liquid surface and R_1 and R_2 are the principal radii of surface curvature[44].

$$\Delta P = \gamma \left(\frac{1}{R_1} + \frac{1}{R_2} \right) \text{ (Eq. 1)}$$

Flocculation analysis

20 ml suspensions were prepared using 2.5 vol% Mg(OH)₂ and milli-Q water and then sonified for 20 minutes to breakup any preformed aggregates. Varying concentrations of polymer between 25ppm and 3000 ppm were then added from a 10000 ppm bulk solution and agitated using a magnetic stirrer for 20 minutes. The Mg(OH)₂-polymer suspensions were then added to a Malvern Mastersizer 2000E (Malvern Panalytical Ltd) SLS particle size analyser dispersion unit prefilled with the required surfactant concentration. The dispersion unit was run at 900 rpm to ensure constant shear rates on the aggregated particulates. Floc size distribution data and fractal dimensions were generated from the Mastersizer 2000E by Mie theory based SLS. For determination of the fractal dimension, a particle that satisfies the Rayleigh-Gans-Debye criteria[45] can be characterised by utilising the scattering wave vector Q (a reciprocal of the particle size), the scattering intensity I(Q) and S(Q) (the interparticle structure factor which describes the interference proposed by the primary particles within the aggregate) as proportionalities. For a detailed analysis of light scattering theory within aggregates, see Sorensen [46]. The proportionality in equation 2 therefore can be used to calculate the fractal dimension of the flocs by plotting logI(Q) with respect to logQ[46] as per the following proportionality in Eq. 2[47].

$$I(Q) \propto S(Q) \propto Q^{-d_f} \text{ (Eq. 2)}$$

Floation experiments

A bespoke floation cell (210 ml, 65 mm ID; figure 8) was manufactured with an air inlet and a fritted glass base. 12.31 g of Mg(OH)₂ was added to a measuring cylinder and dosed with 98 μ M of MIBC, the required dose of diblock copolymer and then made up to 210ml with milli-Q water. The cell was stirred for 20 minutes at 250 rpm to facilitate adequate adsorption of copolymer to Mg(OH)₂ surface.

Airflow into the bottom of the cell was set at 0.1 l.min⁻¹ and the agitator speed was reduced to 100 rpm to suspend larger particulates but minimise turbulence in the cell preventing bubble disengagement. Foam generated above the air water interface poured through the outlet at the top of the vessel and into a pre-weighed aluminium collection container. This container was placed into an oven for 24 hours to evaporate the water component of the foam, leaving behind the recovered particulates. The container was then weighed to determine the following performance indicators:

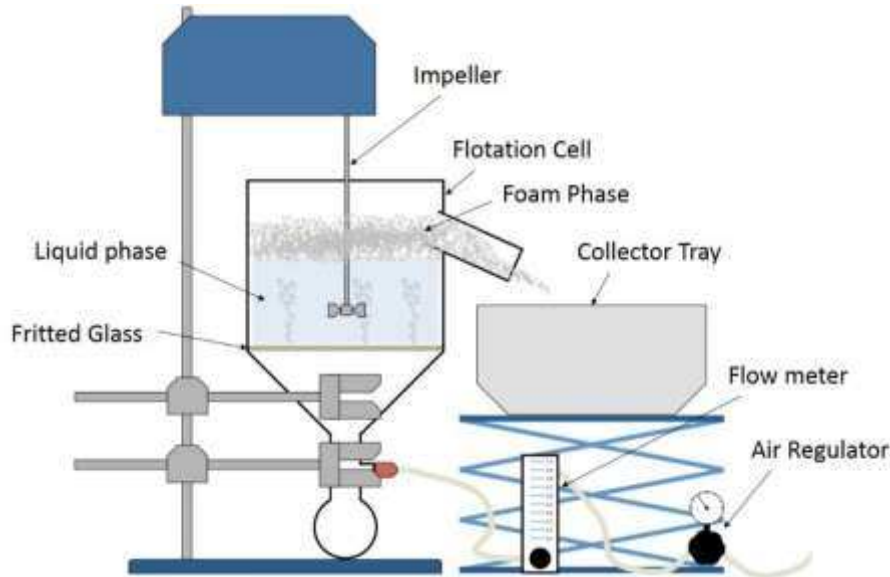


Fig. 8. Illustration of the setup for batch flotation experiments.

Recovery Percentage ($R_{\%}$)

$$R_{\%} = \left(\frac{M_{r,p}}{M_{T,p}} \right) \times 100\% \quad (Eq. 3)$$

The recovery percentage is shown in equation 3, where the recovery percentage, $R_{\%}$, from $Mg(OH)_2$ suspensions as suggested by Zhang et al.[48] is the percentage of the mass of $Mg(OH)_2$ recovered from the initial suspension in the foam phase and the total initial mass of $Mg(OH)_2$ in the flotation cell suspension. $M_{r,p}$ is the recovered mass of $Mg(OH)_2$ from flotation operations and $M_{T,p}$ is the total initial mass of $Mg(OH)_2$ in the system.

Residual Volumetric Concentration ($\xi_{\%}$)

$$\xi_{\%} = \frac{V_{c,p}}{V_{c,f}} \times 100\% = \frac{(M_{T,p} - M_{r,p})}{\rho_p (V_T - V_r)} \times 100\% \quad (Eq. 4)$$

Derived from a material balance of the flotation cell, the residual volumetric concentration shown in equation 4, $\xi_{\%}$, is a fraction of the volume of residual $Mg(OH)_2$ particles in the flotation cell suspension, $V_{c,p}$, and the remaining cell suspension volume post flotation $V_{c,f}$. The residual mass is then divided by the density of $Mg(OH)_2$ (2344 g.l⁻¹) to compute a volume (ρ_p). This is then divided by the remaining volume in the system which is the difference between the initial volume of solids, V_T , and the recovered volume of collapsed foam V_r .

Volume Reduction Factor (V_{red})

$$V_{red} = \left(\frac{V_T}{V_r} \right) \quad (Eq. 5)$$

V_{red} is the volume reduction factor suggested by Mahmoud et al.[49] where V_T is the total volume of the suspension (210ml) and V_r is the volume of extracted suspension i.e. collapsed foam. A larger reduction factor with high floatation yield is favourable, as this means that a large number of particulates have been extracted whilst minimalizing the entrainment of fluid.

RESULTS & DISCUSSION

The change in interfacial surface tension with varying diblock copolymer concentration was analysed using a tensiometer as shown in Figure 9. The PAA₁₅₂-b-PnBA₂₅ copolymer reduced the surface tension of water to a much greater degree than PAA₁₅₂-b-PnBA₂₀₀, a phenomenon previously noted by Colombani et al.[38]. It is likely that steric restrictions prevent larger polymers occupying the air water interface reducing the degree of PAA₁₅₂-b-PnBA₂₀₀ copolymer adsorption. This limit in surface tension reduction is also indicated by the surface tension plateau at ~500 ppm which traditionally indicates the formation of self-assembled micelles to reduce the free energy in the system[50]. At higher concentrations, the air-water interface copolymer adsorption dominates and begins to lower surface tension below that of water. It can be expected that the lower MW PAA₁₅₂-b-PnBA₂₅ will produce greater foaming due to the more pronounced effect on surface tension at concentrations greater than the maximum particle surface adsorption and below its apparent CMC (~1500 ppm). This additional foaming may lead to further fluid entrainment in the foam phase which is known to be potentially detrimental to flotation performance[13]. Further examination of the copolymer self-assembly is required to definitively locate the CMC using techniques such as dynamic light scattering (DLS), but plateaus in surface tension are a fair indication of this mechanism occurring.

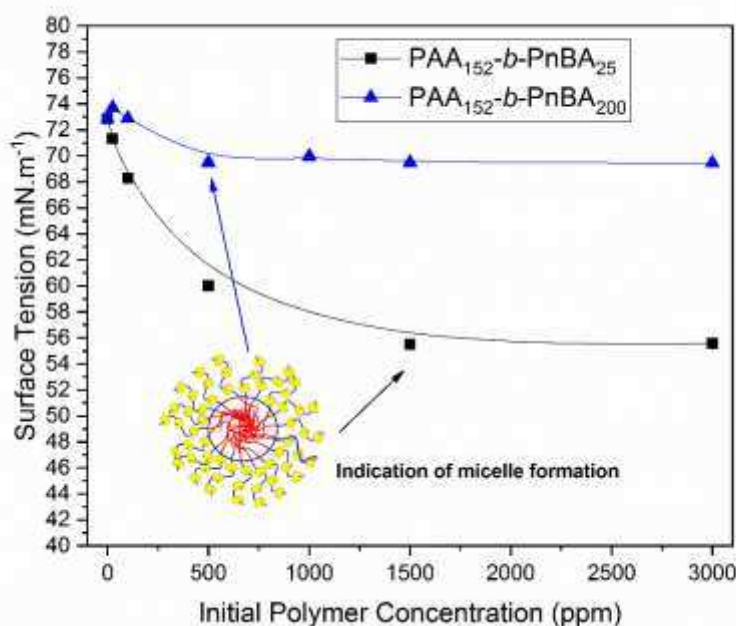


Fig. 9. Change in interfacial surface tension plotted against diblock copolymer concentration for PAA₁₅₂-b-PnBA₂₅ and PAA₁₅₂-b-PnBA₂₀₀ at concentrations 25-3000 ppm.

The resultant floc structure was characterised using SLS, where Figure 10A shows the change in hydrodynamic radii with increasing dose of copolymer for both copolymer systems benchmarked against the aggregation behaviour of SDS surface modified Mg(OH)₂.

The hydrodynamic radii of $\text{Mg}(\text{OH})_2$ flocculated with $\text{PAA}_{152}\text{-b-PnBA}_{25}$ consistently increases with increasing copolymer dose, actively demonstrating flocculation of $\text{Mg}(\text{OH})_2$. Whilst the system flocculated with $\text{PAA}_{152}\text{-b-PnBA}_{200}$ also shows an increase in hydrodynamic radii, to a greater degree than $\text{PAA}_{152}\text{-b-PnBA}_{25}$, the hydrodynamic diameter of the flocs peaks at 500 ppm then plateaus beyond this point at $\sim 18 \mu\text{m}$. When considering the behaviour of the surface tension in Figure 9, it is likely that at concentrations above the CMC, micellar adsorption to the $\text{Mg}(\text{OH})_2$ surface is occurring, which while still promoting flocculation, will limit flocculation performance as whilst the exposed ionic polymer block may adsorb to particle surfaces - promoting charge patch flocculation, the shielded hydrophobic blocks within the micelle structure would not facilitate hydrophobization. SDS initially increases the hydrodynamic diameter of $\text{Mg}(\text{OH})_2$ aggregates, but unlike the diblock copolymers, which induce flocculation, the partial coverage of $\text{Mg}(\text{OH})_2$ surfaces with anionic surfactants will increase the surface energy encouraging aggregation of $\text{Mg}(\text{OH})_2$ [16]. At higher concentrations, the hydrodynamic diameters plateau at the initial particle size indicating that bilayer surfactant coverage which stabilises the colloids and prevents further colloidal aggregation.

SLS also allows for fractal dimension analysis of the copolymer flocs as shown in Figure 10B. The flocs for both polymer systems indicated relatively high fractal dimensions (~ 2.4), which have been associated to smaller denser flocs exhibited in charge patch neutralisation flocculation[21] which was expected from such high charge density hydrophilic polymer blocks. The higher fractal dimension and lower porosity indicates that less fluid will be entrapped within these structures reducing concentrate dilution effects observed by Ng et al[36]. and Forbes et al.[35]. The Mastersizer dispersion unit was run at 900 rpm, this shear is not analogous to that experienced by suspensions in the experimental flotation cell. It is known that excessive shear may reduce floc size[23], [26], [51] and Figure 10C shows a photographic image of flocs remaining in the flotation cell post-flotation - which are visibly larger than the micron scale. Particle size analysis using in-situ or low shear ex situ techniques should be utilised to further characterise these systems. However, SLS sufficiently indicates the presence of flocculation in these systems, but it should be noted that the extent of flocculation is likely greater in the experimental flotation cell which is important for dewatering performance when regarding hydrodynamic limitations[29], [35], [52].

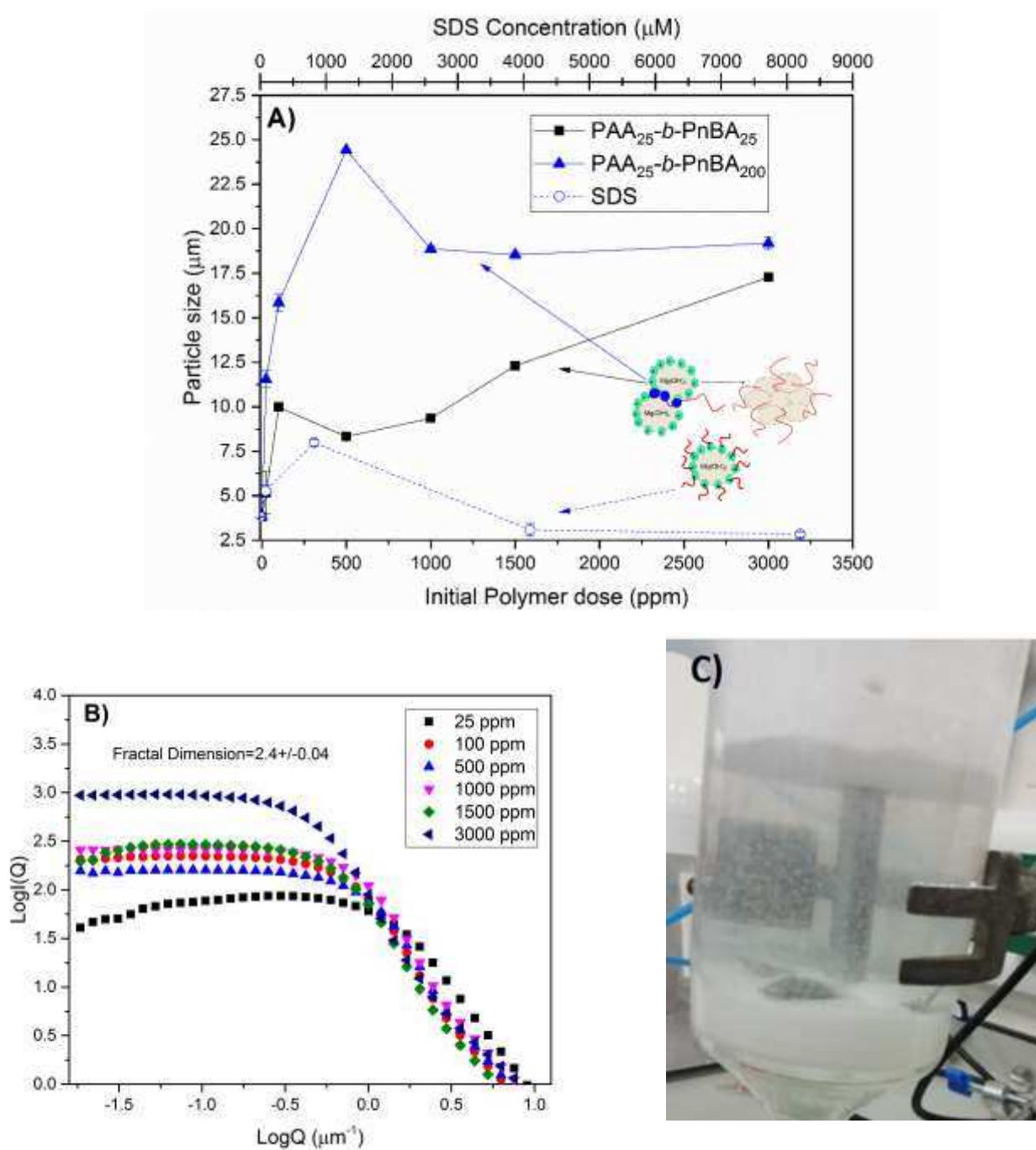


Fig. 10. A) SLS analysis of the change in 50th cumulative percentile floc size with varying concentrations of diblock copolymers and SDS. B) SLS fractal dimension analysis of diblock copolymers. C) Photo of flocs post flotation showing flocs that are visibly larger than the micron scale.

Figure 11 shows the percentage recovery of particles in terms of mass extracted from the experimental flotation cell in the foam phase. SDS appears to largely outperform both polymer systems with a maximum extraction of 93%. Like the behaviour exhibited in Figure 10A, PAA₁₅₂-b-PnBA₂₅ shows a generally consistent increase with increasing concentration and PAA₁₅₂-b-PnBA₂₀₀ increases to a peak at 500 ppm extracting ~52% of Mg(OH)₂ particulates in the suspension. At higher concentrations the performance of PAA₁₅₂-b-PnBA₂₀₀ decreases until essentially being ineffective at floating Mg(OH)₂.

This is potentially a function of micelle formation and adsorption kinetics, where at high concentrations (1000-3000 ppm) the kinetics of micelle formation are so high that these particles are what are primarily adsorbed to the surface of the $Mg(OH)_2$. Whilst still inducing flocculation as shown in Figure 10A, the shielding of the hydrophobic tails within the micelle structure prevent the hydrophobization of these flocs- thus making them incompatible with flotation technology[53]. Given the rate of extraction with increasing PAA_{152} - b - $PnBA_{200}$ copolymer dose is much greater from 0-500 ppm than observed by the PAA_{152} - b - $PnBA_{25}$ copolymer, it is likely that the particles extracted in the latter system may not be through primarily hydrophobic interactions, as this lower extraction rate is observed by Lockwood et al.[13] in the entrainment regime of SDS flotation of $Mg(OH)_2$ (80-800 μM). Additionally, the flotation performance of PAA_{152} - b - $PnBA_{200}$ may not be hydrophobically limited but hydrodynamically limited, as Figure 10C shows images of flocs that are visibly larger than 150 μm which theoretically would be incompatible with bubble attachment due to their large size[30]–[32]. Further investigation with larger hydrophobic block lengths are required to confirm whether these flocs are hydrophobically or hydrodynamically limited in terms of floatability.

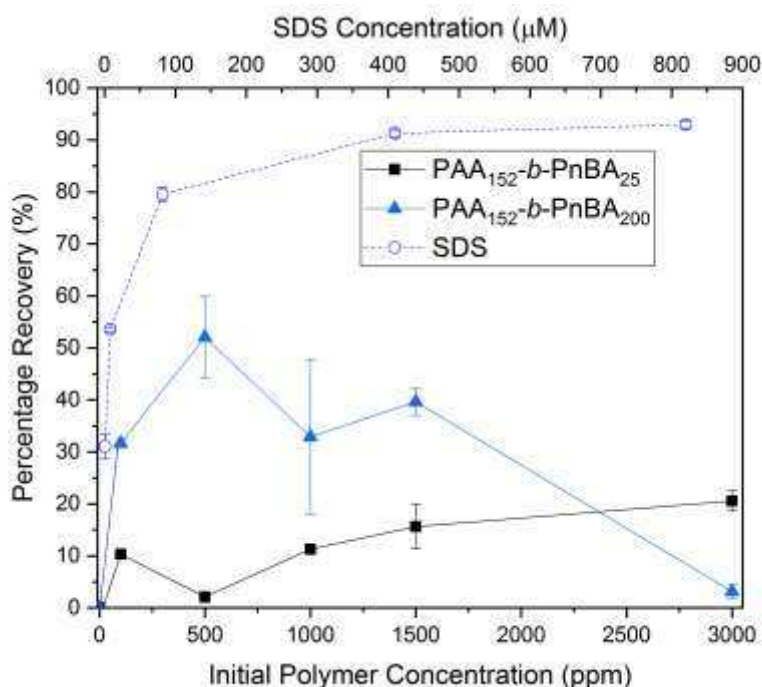


Fig. 11. Percentage recovery of $Mg(OH)_2$ particulates in regards to mass with increasing concentration of PAA_{152} - b - $PnBA_{25}$ and PAA_{152} - b - $PnBA_{200}$ diblock copolymers, benchmarked against SDS performance observed by Lockwood et al.[13].

Figure 12 shows the variation in volume reduction factor (VRF) with different concentrations of diblock copolymer and SDS in the flotation cell. Whilst the data appears to be noisy for both diblock copolymers, it is simply an artefact of the mathematics determining the VRF. If a system effectively retains water, then small variations in carryover translate as large changes in VRF. An important observation is that the largest copolymer, PAA_{152} - b - $PnBA_{200}$ remains constant (relative to the other 2 systems) which is expected as the variation in surface tension with increasing copolymer dose in figure 9 is shown to be minimal, indicating that excess copolymer concentrations do not affect the amount of foaming which is primarily controlled by the frother agent MIBC in these systems. PAA_{152} - b - $PnBA_{25}$ however does show a trend of decreasing VRF with increasing dose of polymer, which like the larger polymer can be attributed to the surface tension data in Figure 9.

The effects are not as drastic as those observed by SDS in the work by Lockwood et al.[13], but still do indicate that fluid entrainment may still be present in the PAA₁₅₂-b-PnBA₂₅ system hindering performance.

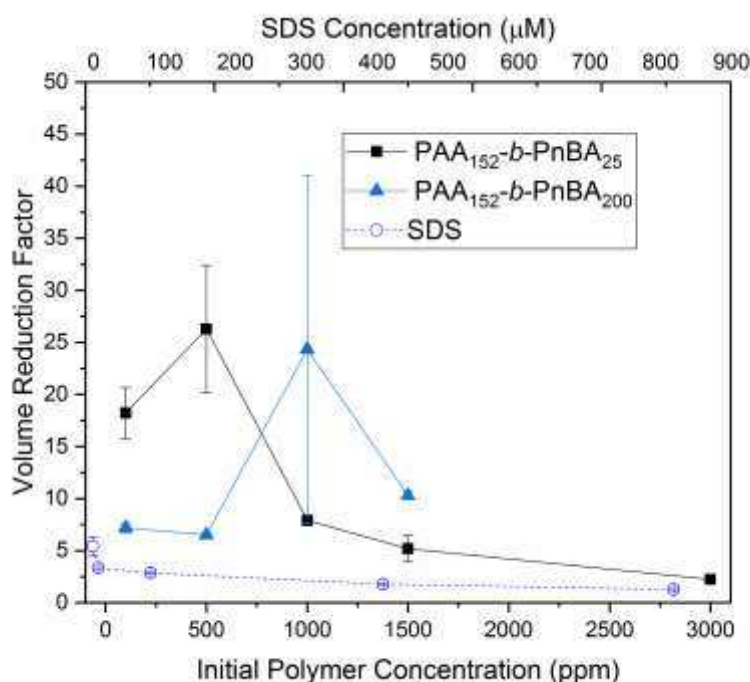


Fig. 12. The volume reduction factor (VRF) of flotation operations using both PAA₁₅₂-b-PnBA₂₅ and PAA₁₅₂-b-PnBA₂₀₀ diblock copolymers as flocculation-flotation aids with varying copolymer concentrations- benchmarked against SDS flotation as observed by Lockwood et al.[13].

Figure 13 shows the residual Mg(OH)₂ volumetric concentration in the flotation cell post-flotation. PAA₁₅₂-b-PnBA₂₅ shows an initial decrease in residual bulk concentration followed by a steady increase in concentration to above the initial suspension concentration of 2.5 vol%. This indicates that the excess foaming caused by the PAA₁₅₂-b-PnBA₂₅ copolymer entrained so much fluid, coupled with the low Mg(OH)₂ particulate recovery recorded in figure 11, that the bulk suspension concentration of Mg(OH)₂ actually increased. As figure 10A showed that the PAA₁₅₂-b-PnBA₂₅ copolymer acted as an effective flocculant at all concentrations of copolymer (25-3000ppm), it is likely that the length of the hydrophobic PnBA block did not provide effective enough hydrophobization of the flocs for bubble attachment. Instead being too effective at encouraging foaming which results in low particle bubble attachment with most of the particulates being extracted via entrainment. PAA₁₅₂-b-PnBA₂₀₀ effectively removed particulates with minimalised foaming to reduce the residual bulk suspension concentration effectively up to the systems apparent CMC (500 ppm), whereas observed in figure 11, the performance decreased with increasing dose likely due to micellar adsorption preventing hydrophobic bubble-particle attachment. The SDS system observed by Lockwood et al.[13] demonstrated similar behaviour reducing the residual cell bulk concentration until a point where fluid entrainment dominates - resulting in a bulk residual concentration increase. Comparatively to the PAA₁₅₂-b-PnBA₂₀₀ system, the SDS appears to perform best based on a dosage basis, however it is likely these better decontamination concentrations are only present with large fluid carry over from the flotation cell.

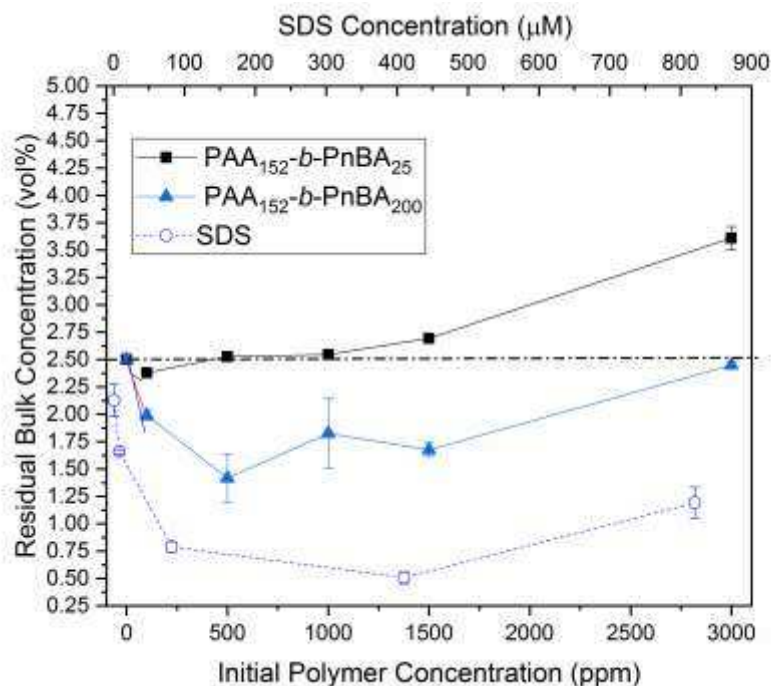


Fig. 13. Residual flotation cell bulk concentration on a volumetric basis with varying diblock copolymer and SDS concentrations as observed by Lockwood et al.[13].

Analysis of the comparative flotation performance of the SDS system investigated by Lockwood et al.[13] and the PAA₁₅₂-b-PnBA₂₀₀ diblock copolymer as conducted shown in Figures 14A and B, where the analysis was completed on a percentage recovery basis rather than surfactant/copolymer concentration basis. Figure 14A shows the residual bulk concentration as a function particulate recovery for the two systems. Figure 14A shows that for the equivalent extraction of particles, the SDS system is less effective at reducing the residual bulk concentration than PAA₁₅₂-b-PnBA₂₀₀, this coupled with the analysis in figure 14B, which displays the remaining cell volume by percentage as a function of particulate recovery shows that whilst the SDS is separating particulates, the water entrainment associated with this extraction is to a larger degree than that of PAA₁₅₂-b-PnBA₂₀₀. At extraction above the maximum attained by PAA₁₅₂-b-PnBA₂₀₀, the additional particulate extraction achieved by SDS is associated with very large fluid carryover during flotation. This is demonstrated by observing the maximum particle extraction of 93% is associated with 79% fluid loss by volume, which is not an effective solid-liquid separation operation for the nuclear industry- as this will translate to a reduction in waste packaging efficiency which will increase the cost of final disposal.

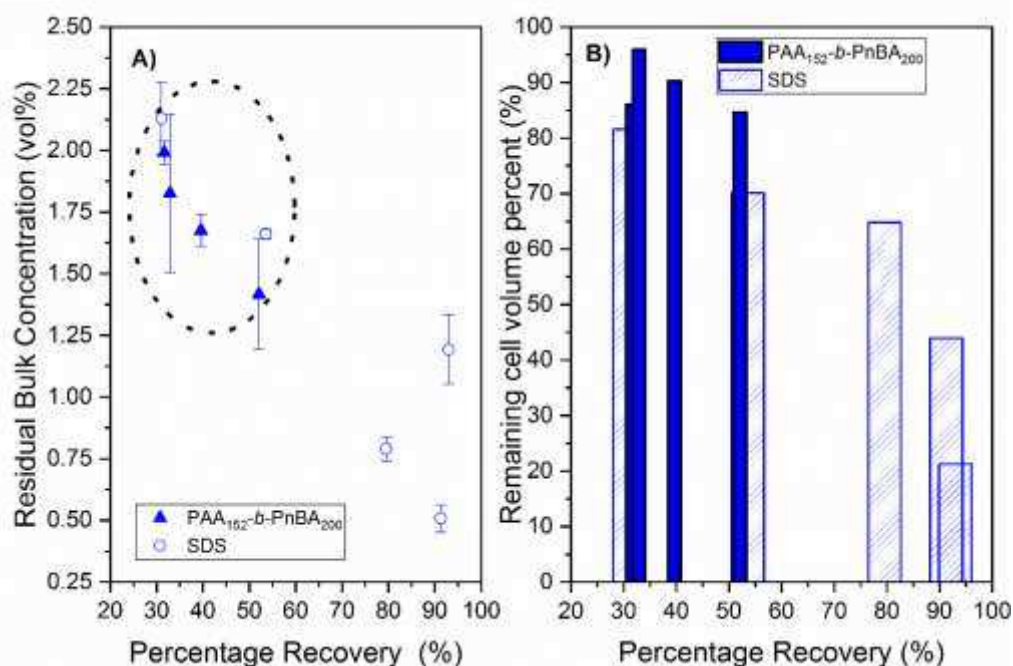


Fig. 14. A) Dewatering performance of PAA₁₅₂-b-PnBA₂₀₀ and SDS on a percentage recovery basis.
 B) Remaining cell volume percentage of the PAA₁₅₂-b-PnBA₂₀₀ and SDS flotation systems as a function of particle percentage recovery.

The potential for the use of diblock copolymers has been successfully demonstrated in this research as an alternative to traditional surfactant systems for rapid flotation separation. The length of the hydrophobic block was observed to critically affect the extent of extraction, with the shorter block encouraging additional foaming and thus entrainment, due to its likely higher density adsorption to the air-water interface, while also failing to provide adequate modification to the resultant particle contact angles for compatibility with bubble attachment. The larger hydrophobic block copolymer had little effect on surface tension and thus foamability, whilst effectively flocculating and hydrophobizing Mg(OH)₂. While it is still not fully understood whether the percentage recovery limitation is purely dominated by hydrophobic or hydrodynamic phenomena, further work investigating polymers of larger hydrophobic block length and varying hydrophilic block lengths for control of the particle size distribution is being conducted. Further investigation of the surface chemistry of these polymers is also planned, using techniques such as DLS to determine the CMC of these systems explicitly and more detailed analysis of the dynamic surface interactions using oscillatory surface tension analysis.

It should also be noted that other factors, such as adjusting shear rates experienced by these flocculated suspensions and the strategic implementation of this technology will further affect the overall removal efficiency. For example, the performance of SPP1 could be improved by the application of PAA₁₅₂-b-PnBA₂₀₀ as a flocculating agent to reduce the sedimentation residence time and increase the dewatering capacity of this unit operation. Flotation then, due to its advantages of being a low footprint, high efficiency separation process, could potentially be retrofitted between SPP1 and FGMSF to remove the unsetttable material being returned to the pond, where the now flocculated fine material can be extracted through flotation with minimal additional fluid loss to improve the separation extent of radionuclide carrying Mg(OH)₂ colloids.

These copolymers have therefore demonstrated their potential as an effective tool in reducing the decontamination burden on downstream processes, which ultimately could decrease site radiological discharges to the environment helping to justify nuclear energy as a viable method of combatting climate change in the UK, without the stigma of its environmental impact regarding waste.

CONCLUSIONS

Diblock copolymers are evaluated as dual flocculation and collector agent for flotation operations and benchmarked against the minerals industry surfactant-based collector agent, SDS for flotation separation. Flotation performance limitations are often attributed to failure to extract ultra-fine material (<20 µm)[30]–[32] due to issues negotiating slip streams created by rising bubbles. In this research, two diblock copolymers synthesized using reversible addition chain fragmentation (RAFT) polymerisation from acrylic acid and n-butyl acrylate to form poly(acrylic acid)-block-poly(n-butyl acrylate). The hydrophobic poly(acrylic acid) block was held constant at a degree of polymerisation of 152 and the length of the hydrophobic poly(n-butyl acrylate) blocks for the two copolymers were synthesised at degrees of polymerisation of 25 and 200. Due to the segregation of the monomers, the diblock copolymers displayed surfactant like behaviour, modifying the surface tension of aqueous media. It was found that the smaller hydrophobic chain length polymer, Dp=25, lowered the surface tension of water to a greater degree than the larger copolymer, Dp=200, and appeared to form self-assemble micelle particles at a higher concentration than the larger polymer (~500 ppm). Both polymers successfully demonstrated flocculation of Mg(OH)₂ suspensions forming charge patch neutralisation flocs unlike previous literature on statistical copolymers which form larger bridging flocs which were found to entrain gangue material. However, it was noted that the larger polymer at concentrations above its critical micelle concentration may exhibit micellular adsorption hindering its effectiveness as a flotation aid. This was further confirmed when analysing the flotation performance. The effectiveness of flotation of these systems was completed by investigating three properties, the percentage particle recovery as a function of mass, the volume reduction factor and the residual flotation cell particle concentration in terms of volume. It was found that the larger copolymer performed better than the smaller polymer removing a maximum of 52% of particulates below its CMC and retained the most water in the flotation cell. This performance was compared on a recovery percentage basis to SDS, which had been found to extract a maximum of 93% of particulates but at the cost of 79% of the initial fluid volume. When comparing on a percentage extraction basis, the copolymer outperformed the SDS system up until its maximum extraction of 52% producing a lower residual flotation cell particulate concentration. Further work is required to determine whether the copolymers are hydrodynamically or hydrophobically limited, with the implementation of additional diblock copolymers with varying hydrophobic and hydrophilic chain lengths planned.

ACKNOWLEDGEMENTS

The authors would like to thank the Engineering and Physical Sciences Research Council (EPSRC) U.K and Sellafield Ltd for funding this research through the Centre for Doctoral training in Next Generation Nuclear (NGN-CDT) [EP/L01539011].

REFERENCES

- (1) Jackson, S. F.; Monk, S. D.; Riaz, Z. An investigation towards real time dose rate monitoring, and fuel rod detection in a first generation magnox storage pond (FGMSP). *Appl. Radiat. Isot.* **2014**, 94, 254–259.
- (2) Hallam, K. R.; Minshall, P. C.; Heard, P. J.; Flewitt, P. E. J. Corrosion of the alloys magnox al80, magnox zr55 and pure magnesium in air containing water vapour. *Corros. Sci.* **2016**, 112, 347–363.

- (3) Heath, P. G.; Stewart, M. W. A.; Moricca, S.; Hyatt, N. C. Hot-isostatically pressed wastefoams for magnox sludge immobilisation. *J. Nucl. Mater.* **2018**, 499, 233–241.
- (4) Barlow, S. T.; Stennett, M. C.; Hand, R. J.; Morgan, S. P.; Hyatt, N. C. Thermal treatment of UK magnox sludge. In 2nd Petrus-OPERA PhD and early stage researcher conference 2016 ; 2016.
- (5) Richardson, A.; Maher, P. Sellafield fuel handling plant pondwater update NuSAC(04)P17. (Update of NuSAC(03)P10) <http://www.hse.gov.uk/aboutus/meetings/iacs/nusac/051104/p10.pdf> (accessed Jun 16, 2018).
- (6) Maher, Z.; Ivanov, P.; O'Brien, L.; Sims, H.; Taylor, R. J.; Heath, S. L.; Livens, F. R.; Goddard, D.; Kellet, S.; Rand, P.; et al. Americium and plutonium association with magnesium hydroxide colloids in alkaline nuclear industry process environments. *J. Nucl. Mater.* **2016**, 468, 84–96.
- (7) Woods, R.-M.; Gunter, M. E. Na- and Cs-Exchange in a Clinoptilolite-rich rock: analysis of the outgoing cations in solution. *Am. Mineral.* **2001**, 86 (4), 424–430.
- (8) Grant, I.; Weintrager, U.; Richardson, I. E.; Wilson, D. Sellafield FGMSP additional sludge retrievals a significant step in decommissioning part of the U.K.'s nuclear legacy -16180. In Waste Management Symposium; Phoenix, Arizona, USA, 2016.
- (9) Hogg, R. Flocculation and dewatering. *Int. J. Miner. Process.* **2000**, 58 (1–4), 223–236.
- (10) Al-Naafá, M. A.; Selim, M. S. Sedimentation of polydisperse concentrated suspensions. *Can. J. Chem. Eng.* **1989**, 67 (2), 253–264.
- (11) van Deventer, B. B. G.; Usher, S. P.; Kumar, A.; Rudman, M.; Scales, P. J. Aggregate densification and batch settling. *Chem. Eng. J.* **2011**, 171 (1), 141–151.
- (12) Brazil, B. L.; Summerfelt, S. T. Aerobic treatment of gravity thickening tank supernatant. *Aquac. Eng.* **2005**, 34 (2), 92–102. <https://doi.org/10.1016/j.aquaeng.2005.06.001>.
- (13) Lockwood, A. P. G.; Kok Shun, P.; Harbottle, D.; Warren, N. J.; Randall, G.; Peakall, J.; Hunter, T. N. Dissolved air flotation for rapid dewatering and separation of legacy sludge wastes. In Waste Management Symposium; Phoenix, Arizona, USA, 2019.
- (14) Johnson, M.; Peakall, J.; Fairweather, M.; Biggs, S.; Harbottle, D.; Hunter, T. N. Characterization of multiple hindered settling regimes in aggregated mineral suspensions. *I&EC Res.* **2016**, 55, 9983–9993.
- (15) Hogg, R. Bridging flocculation by polymers. *KONA Powder Part. J.* **2013**, 30, 3–14.
- (16) Gregory, J.; Barany, S. Adsorption and flocculation by polymers and polymer mixtures. *Adv. Colloid Interface Sci.* **2011**, 169 (1), 1–12.
- (17) Nasser, M. S.; James, A. E. The effect of electrolyte concentration and pH on the flocculation and rheological behaviour of kaolinite suspensions. *J. Eng. Sci. Technol.* **2009**, 4 (4), 430–446.
- (18) Nasser, M. S.; James, A. E. The effect of polyacrylamide charge density and molecular weight on the flocculation and sedimentation behaviour of kaolinite suspensions. *Sep. Purif. Technol.* **2006**, 52 (2), 241–252.
- (19) Heath, A. R.; Bahri, P. A.; Fawell, P. D.; Farrow, J. B. Polymer flocculation of calcite: relating the aggregate size to the settling rate. *AIChE J.* **2006**, 52 (6), 1987–1994.
- (20) Witham, M. I.; Grabsch, A. F.; Owen, A. T.; Fawell, P. D. The effect of cations on the activity of anionic polyacrylamide flocculant solutions. *Int. J. Miner. Process.* **2012**, 114–117, 51–62.
- (21) Zhou, Y.; Franks, G. V. Flocculation mechanism induced by cationic polymers investigated by

- light scattering. *Langmuir* **2006**, 22 (16), 6775–6786. <https://doi.org/10.1021/LA060281+>.
- (22) Sharma, S. Lin, C, Miller, J, D. Multi-scale features including water content of polymer induced kaolinite floc structures. *Miner. Eng.* **2017**, 101, 20–29.
- (23) Lu, C. F.; Spielmant ', L. A. Kinetics of floc breakage and aggregation in agitated liquid suspensions. *Colloid Interface Sci.* **1985**, 103 (1).
- (24) Vajihinejad, V.; Soares, J. B. P. Monitoring polymer flocculation in oil sands tailings: a population balance model approach. *Chem. Eng. J.* **2018**, 346, 447–457.
- (25) Kyoda, Y.; Costine, A. D.; Fawell, P. D.; Bellwood, J.; Das, G. K. Using focused beam reflectance measurement (FBRM) to monitor aggregate structures formed in flocculated clay suspensions. *Miner. Eng.* **2019**, 138, 148–160.
- (26) Maggi, F. Variable fractal dimension: a major control for floc structure and flocculation kinematics of suspended cohesive sediment. *J. Geophys. Res. Ocean.* **2007**, 112 (7), 1–12.
- (27) Franks, G. V; Yates, P. D.; Lambert, N. W. A.; Jameson, G. J. Aggregate size and density after shearing, implications for dewatering fine tailings with hydrocyclones. *Int. J. Miner. Process.* **2005**, 77 (1), 46–52.
- (28) Teixeira, M. R.; Rosa, M. J. Comparing dissolved air flotation and conventional sedimentation to remove cyanobacterial cells of *microcystis aeruginosa*: part i: the key operating conditions. *Sep. Purif. Technol.* **2006**, 52 (1), 84–94.
- (29) Ng, W. S.; Connal, L. A.; Forbes, E.; Franks, G. V. A review of temperature-responsive polymers as novel reagents for solid-liquid separation and froth flotation of minerals. *Miner. Eng.* **2018**, 123, 144–159.
- (30) Fuerstenau, M.C.; Jameson, G.; Yoon, R. *Froth Flotation: A Century of Innovation*; 2007.
- (31) Gaudin, A. M.; Schuhmann, R.; Schlechten, A. W. Flotation Kinetics. II. The effect of size on the behavior of galena particles. *J. Phys. Chem.* **1942**, 46 (8), 902–910.
- (32) Norori-McCormac, A.; Brito-Parada, P. R.; Hadler, K.; Cole, K.; Cilliers, J. J. The effect of particle size distribution on froth stability in flotation. *Sep. Purif. Technol.* **2017**, 184, 240–247.
- (33) De F. Gontijo, C.; Fornasiero, D.; Ralston, J. The limits of fine and coarse particle flotation. *Can. J. Chem. Eng.* **2008**, 85 (5), 739–747.
- (34) Ng, W. S.; Cooper, L.; Connal, L. A.; Forbes, E.; Jameson, G. J.; Franks, G. V. Tuneable collector/depressant behaviour of xanthate-functional temperature-responsive polymers in the flotation of copper sulfide: effect of shear and temperature. *Miner. Eng.* **2018**, 117, 91–99.
- (35) Forbes, E.; Bradshaw, D.; Franks, G. Temperature sensitive polymers as efficient and selective flotation collectors. *Miner. Engineering* **2011**, 24 (8), 772–777.
- (36) Ng, W. S.; Sonsie, R.; Forbes, E.; Franks, G. V. Flocculation/flotation of hematite fines with anionic temperature-responsive polymer acting as a selective flocculant and collector. *Miner. Eng.* **2015**, 77, 64–71.
- (37) Stitt, C. A.; Harker, N. J.; Hallam, K. R.; Paraskevoulakos, C.; Banos, A.; Rennie, S.; Jowsey, J.; Scott, T. B. An investigation on the persistence of uranium hydride during storage of simulant nuclear waste packages. *PLoS One* **2015**, 10 (7).
- (38) Colombani, O.; Ruppel, M.; Schubert, F.; Zettl, H.; Pergushov, D. V.; Müller, A. H. E. Synthesis of Poly(n -Butyl Acrylate)- Block -Poly(Acrylic Acid) diblock copolymers by atrp and their micellization in water. *Macromolecules* **2007**, 40 (12), 4338–4350.

- (39) Evans, L.; Paul Thalody, B.; Morgan, J. D.; Nicol, S. K.; Napper, D. H.; Warr, G. G. Ion flotation using carboxylate soaps: role of surfactant structure and adsorption behaviour. *Colloids Surfaces A Physicochem. Eng. Asp.* **1995**, 102 (C), 81–89.
- (40) Versamag Mg(OH)₂ MSDS. Martin Marietta Magnesia Specialties 2016.
- (41) IXOM. Methyl Isobutyl Carbinol MSDS; 2017.
- (42) Perrier, S. 50th anniversary perspective: raft polymerization - a user guide. *Macromolecules. American Chemical Society* October 10, 2017, pp 7433–7447.
- (43) Lovett, J. R.; Warren, N. J.; Armes, S. P.; Smallridge, M. J.; Cracknell, R. B. Order–order morphological transitions for dual stimulus responsive diblock copolymer vesicles. *Macromolecules* **2016**, 49 (3), 1016–1025.
- (44) Ranjbar, H.; Khosravi-Nikou, M. R.; Safiri, A.; Bovard, S.; Khazaei, a. Experimental and theoretical investigation on nano-fluid surface tension. *J. Nat. Gas Sci. Eng.* **2015**, 27, 1806–1813.
- (45) Glover, S. M.; Yan, Y.; Jameson, G. J.; Biggs, S. Bridging flocculation studied by light scattering and settling. *Chem. Eng. J.* **2000**, 80 (1–3), 3–12.
- (46) Sorensen, C. M. Light scattering by fractal aggregates: a review. *Aerosol Sci. Technol. Am. Assoc. Aerosol Res.* **2001**, 35, 648–687.
- (47) Burns, J. L.; Yan, Y.-D.; Jameson, G. J.; Biggs, S. A light scattering study of the fractal aggregation behavior of a model colloidal system. *Langmuir* **1997**, 13 (24), 6413–6420.
- (48) Zhang, H.; Kim, Y. K.; Hunter, T. N.; Brown, A. P.; Lee, J. W.; Harbottle, D. Organically modified clay with potassium copper hexacyanoferrate for enhanced Cs⁺ adsorption capacity and selective recovery by flotation. *J. Mater. Chem. A* **2017**, 5 (29), 15130–15143.
- (49) Mahmoud, M. R.; Soliman, M. A.; Rashad, G. M. PERFORMANCE appraisal of foam separation technology for removal of Co(II)-EDTA complexes intercalated into in-situ formed Mg-Al layered double hydroxide from radioactive liquid waste. **2017**.
- (50) Pashley, R. M.; Karaman, M. E.; John Wiley & Sons. *Applied colloid and surface chemistry*; J. Wiley, 2004.
- (51) Michaels, A. Bolger, J. Settling rates and sediment volumes of flocculated kaolin suspensions. *I&EC Fundam.* **1962**, 1 (1), 24–33.
- (52) Sung Ng, W.; Connal, L. A.; Forbes, E.; Mohanaragam, K.; Franks, G. V. In situ study of aggregate sizes formed in chalcopyrite-quartz mixture using temperature-responsive polymers. *Adv. Powder Technol.* **2018**, 29 (8), 1940–1949.
- (53) Epple, M.; Schmidt, D. C.; Berg, J. C. The effect of froth stability and wettability on the flotation of a xerographic toner. *Colloid Polym. Sci.* **1994**, 272 (10), 1264–1272.